# A demodulation inductive proximity sensor with suppression of background magnetic flux density

Stefan Hoberg
University of Siegen
Institute of Microsystems Technology (IMT)
Email: stefan.hoberg@uni-siegen.de

Prof. Dr. Dietmar Ehrhardt
University of Siegen
Institute of Microsystems Technology (IMT)
Email: dietmar.ehrhardt@uni-siegen.de

***Abstract*—A novel inductive proximity sensor system is accomplished in this paper. Primarily this system uses a modulated magnetic field generator (modulation of current in a coil) and a lock-in receiver which demodulates the magnetic flux density by using a Hall effect device. In contrast to published sensors this approach increases the signal-to-noise ratio (SNR) by a demodulation and a subsequent integration process which is implemented in the lock-in receiver at an isochronous suppression of DC or AC modulated background magnetic flux density.**
**The performance is predicted by simulation and validated by a demonstrator. It is shown that the demodulation inductive proximity sensor works in a hostile environment in which the amplitude of a background magnetic flux density has a similar (or higher) amplitude compared to the active modulated flux density.**

## I. Introduction

There is a long history of inductive proximity sensing. This kind of sensor systems have been part of research for many years. An inductive sensor system generates a magnetic flux which interacts with a target (metal or graphite) and causes eddy currents in the surface of this target. The eddy currents themselves dissipate power due to the resistance of the target, leading to an increased temperature. Also the eddy currents cause a second magnetic flux density which overlays to the original one but with different phase and amplitude. The characteristic of how the original field is distorted by the superposition results in an information about the position and the material properties respectively. Usually these sensors are applied in the domains of contactless sensing (proximity sensing) and non-destructive material investigation. In the field of proximity sensing distances of conductive surfaces and rotations relative to the sensor have to be detected in a hostile environment. Current linkage from power supplies, which may be DC or AC, are influencing the performance of inductive sensors. Herein lies the challenge.

There are proximity sensors in the market that differ in three fundamental techniques. One classic approach uses an oscillator. A LC tank operates in oscillation state. If eddy currents flow in the target, the energy in the magnetic field is decreased and attenuates the oscillator, whereby the oscillations stop. A more sophisticated sensor system uses an approach similar to the transformer principle. Only the mutual inductance is influenced by the target which results in material independent detection. The mutual inductance is constant independent of the target material. Another system uses a pulse approach in which broad spectral signals are applied to the target. The advantage of this is that besides the independence of the target material, influence due to temperature drifts are minimized and the sensitivity can be increased compared to the both described before. Common to all three systems is that the transmitter and receiver consists of the same coil. The sensitivity to distortions is at a maximum when high frequency fields appear due to induction. None of those systems are able to sense in a hostile environment in which the background magnetic flux density has the same or a higher amplitude than the active flux density has. Especially due to the induction already low amplitudes at higher frequencies (10kHz to GHz) affect the performance of these sensors significantly.

In section II a novel approach is outlined, which uses a lock-in receiver to overcome this constrains. The main focus is on theoretical considerations which are supported by simulation results. Section III shows a first demonstrator and describes the system architecture in detail. Results are summarized in section IV. Conclusion and outlook of future proximity sensing with lock-in Hall effect devices are reported in section V.

## II. A theoretical consideration

The ability how effective distortions due to a target can be sensed is an important issue in the development of an inductive proximity sensor. As aforementioned the sensor can be influenced by fields of the environment.

Basically the inductive sensor is modeled like a transceiver system with the coil as the transmitter and the lock-in Hall effect device as the receiver. In fig. 1 the principle setup is shown. A common clock source triggers the transmitter and the receiver with the same frequency. It is important that the frequency dependence between the transmitter and receiver are fixed because hereby the correlation of the incoming superpositioned magnetic flux density and the outgoing magnetic flux density of the transmitter can be calculated. An amplifier in the transmitter is clocked and biases the coil with a modulated current. Neglecting saturation effects the current is proportional in amplitude and phase to the magnetic flux density. Because of induction in the target eddy currents generates a second magnetic field and superposes this to the original. The resulting flux density is demodulated and converted to a voltage signal in the baseband. This signal is

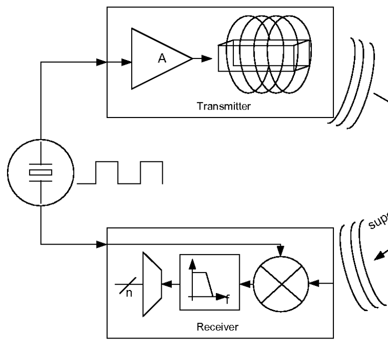


Fig. 1. Basic transceiver principle of a lock-in proximity sensor

integrated over a variable time $t_{int}$ and finally converted into a digital signal.
The question is how can the high mathematical demand of demodulation and integration be processed in a very simple implementation. A Hall effect device can be imagined as a demodulator. A voltage appears transverse to the direction of the current density if a magnetic flux density is applied to a conductive plate (usually a semiconductor plate like Si). A simplified equation for the Hall voltage is

$$V_H = R_H \cdot I_x \cdot B_z \cdot \frac{1}{t} \tag{1}$$

In eq. 1 $R_H$ represents the material properties, t the thickness of the plate, $I_x$ the current orthogonal to the magnetic flux density $B_z$ which are both orthogonal to an electrical field which results in the Hall voltage $V_H$. Herein lies the demodulation ability of a simple piece of silicon. Eq. 1 describes an ideal Hall plate. Effects like offset, noise, geometrical effects, piezo effects, etc. are well known and must be considered in a realization. In a second step the Hall voltage has to be integrated by an electrical circuit.
In a first approach the transmitter is sinusoidal modulated whereby the flux density is continuous and no induction effects appear. The spectrum of the magnetic flux density consists of only the first harmonic. The lock-in receiver is modulated with a square waveform. In fig. 2 are two different cases considered. The signals are plotted over two modulation periods, whereby in the left column the simplest case is shown. In the right column the effects due to a superposition of a DC background magnetic flux density are visible. The sinusoidal modulation signal of the magnetic flux density and the squared modulation signal for the Hall effect device are plotted in rows a) and b). The resulting Hall voltage is plotted in the row c). In the left case the second half period has changed the sign. In the right case this happens to the active modulation part of the magnetic flux density while the DC part doesn't change its sign. It is clear that by means of a temporal integration this DC signal is filtered completely. This behavior is plotted in row d). The fact that Hall effect devices have linear response curves over several decades provides a suppression functionaltity for large background signals. Furthermore every background AC-signals which are different in frequency are filtered. In case

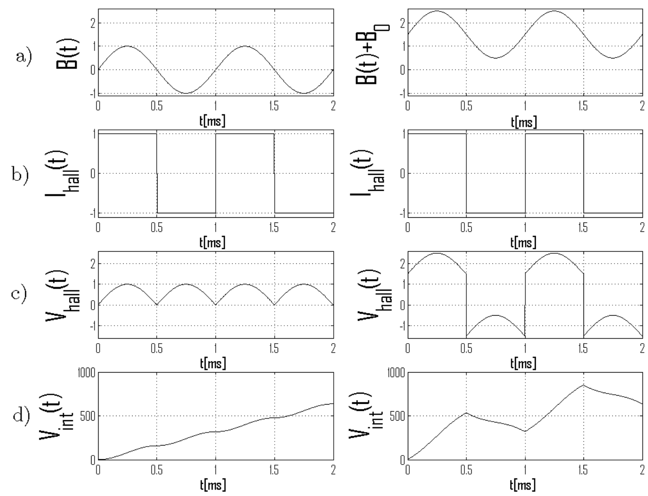


Fig. 2. Theoretical behavior of the lock-in receiver

| | | | |
|---|---|---|---|
| left a) | flux density | right a) | flux density plus DC signal |
| left b) | modulated Hall current | right b) | modulated Hall current |
| left c) | Hall voltage | right c) | Hall voltage |
| left d) | integrated Hall voltage | right d) | integrated Hall voltage |

the background signal frequency is lower than the modulation frequency the integration time has to be a multiple of the period-length of the modulated signal. This results in the temporal integral over the background signal being zero. In case the background signal frequency is higher than the modulation signal frequency the integration time must be one period at least. If the signal frequency is an even multiple of the modulation frequency the integral across the background signal is zero after one modulation period. In other cases than even multiples the integration is continued until the integral of the background signal is zero. The closer the background signal frequency to the modulation frequency is the longer the integration time has to be set.
The information of the environment of the proximity sensor is contained in the superpositioned flux density which is also sinusoidal but different in phase and amplitude to the original flux density. Altogether it contains three unknowns: dc offset, amplitude and phase. The frequency is known and is e. g. 1kHz. To solve this linear equation system three samples per modulation period are necessary [2]. A practical implementation is the trigonometrically interpolation which uses four samples ($a_1$, $a_2$, $a_3$, $a_4$). A 90° shift results in a significant simplification of the computation of the unknowns.

$$\text{dc offset}: \; B_0 = \frac{a_1 + a_2 + a_3 + a_4}{4} \tag{2}$$

$$\text{amplitude}: \; A = \frac{\sqrt{(a_1 - a_3)^2 + (a_2 - a_4)^2}}{4} \tag{3}$$

$$\text{phase}: \; \Phi = \arctan\left(\frac{a_1 - a_3}{a_2 - a_4}\right) \tag{4}$$

Due to the process of demodulation (multiplication) and phase shifting (transmitter or receiver signal shift are equivalent) a

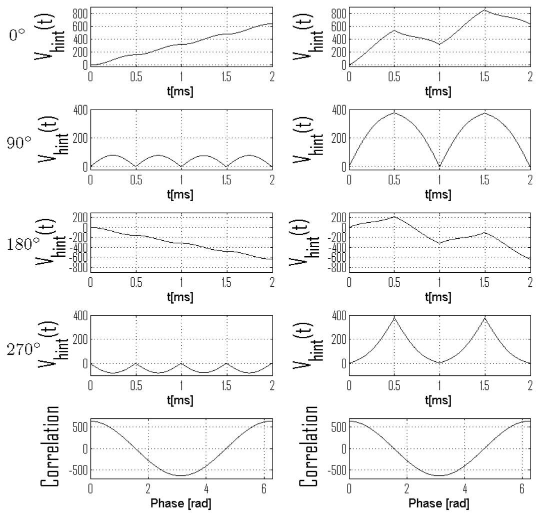

Fig. 3. Trigonometrical interpolation and correlation function
left 0° $V_{int}$, right 0° $V_{int}$ inclusive DC signal
left 90° $V_{int}$, right 90° $V_{int}$ inclusive DC signal
left 180° $V_{int}$, right 180° $V_{int}$ inclusive DC signal
left 270° $V_{int}$, right 270° $V_{int}$ inclusive DC signal

correlation for one period is calculated. In fig. 3 are these samples plotted. As before the basic case is plotted on the left while the superposed signal is on the right. In the first four rows the phase dependend integrated Hall voltages for a phase shift between transmitter and receiver signals are shown. Each voltage is integrated over two periods while the 90° and 270° are zero after each period. With the aid of these samples the correlation can be solved, respectively the unknowns. In the bottom row of each case the correlation function is plotted whereby the phaseshift has a finer resolution (0.5° instead of 90°) to get a more clear plot. This simulation points out that due to the demodulation process the signal is mixed to the baseband (0 Hz) and the subsequent integration operates like a noise filter. It's bandwidth is inversely proportional to the integration time respectively the number of periods. According to the behavior of every mixer (demodulator) all spectral parts are mixed (demodulated) to another frequency. While increasing the integration time more and more spectral parts are filtered beyond the corner frequency of the noise filter.

The integration is important concerning to noise which is part of the Hall voltage at anytime. The signal-to-noise ratio can be affected positively by the choice of modulation frequency and integration time. In [1] the occurring noise magnitudes and their causes are described. One statement is that the noise power spectral density is given by 1/f noise ($S_{Nf}(f)$) and thermal noise ($S_{NT}$). In the lower spectral range $S_{Nf}(f)$ dominates while at higher frequency $S_{NT}$ does. The crossover point is at the corner frequency $f_c$ of $S_{Nf}(f)$. It is obvious that due to the demodulation this spectral noise density is

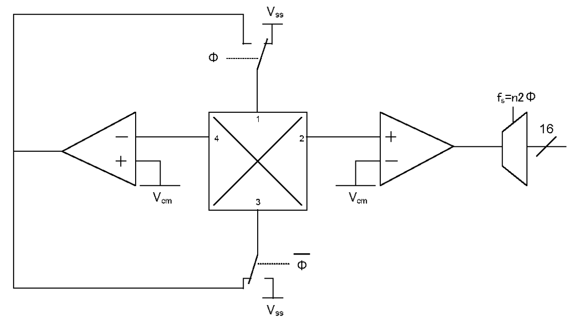

Fig. 4. Schematically illustration of the proximity sensor receiver

altered to another demodulated noise power spectral density. The lower spectral range is dominated by the power spectral density which was originally at the modulation frequency $f_m$. If $f_m > f_c$ is valid, thermal noise appears in the lowest frequency range instead of 1/f noise. Due to the temporal integration the equivalent noise bandwidth is $\frac{1}{2 \cdot t_{\text{int}}}$ [3]. Thus the signal-to-noise ratio increases only at extension of the integration time.

## III. System Architecture

In section II is mentioned that the lock-in receiver consists at least of a Hall effect device, an integrator and an ADC. The transmitter consists of an amplifier which buffers the current of the inductive load. The inductance is 3mH at 1kHz and is wrapped around a half open ferrite core. In first investigations a simple Class AB amplifier is used. The applied frequency range is 1kHz to 20kHz. An implementation of the demodulation proximity sensor is realized on printed circuit board level as shown in fig. 4. The circuit consists of driving and readout electronics. Biasing current of the Hall effect device is supplied by an opamp on the left. The equivalent circuit for the Hall device can be modeled like a resistive bridge circuit. The current causes a voltage drop over the resistances and is available at ports 2 and 4. The regulation due to the opamp on the left side causes that the voltage drop at port 4 equals $V_{CM}$. Due to transmission gates at ports 1 and 3 the current direction is modulated with the frequency of $\Phi$. At port 2 is a Hall voltage referred to $V_{SS}$ available. For a high sensitivity of the Hall effect device the bias current should be as large as possible (see eq. 1) be. This means that the on-resistance (ron) of the transmission gates should be small. Thereby the input resistance dominates the voltage divider which consists of the transmission gates and the Hall effect device. The supply voltage is 5V. This leads to a sensitivity of the Hall device of $0.1\frac{V}{T}$. A standard Hall effect device is used without a boosted sensitivity [7]. The Hall voltage is buffered by a second opamp. The opamp is offset compensated by means of auto zeroing and is adjustable in amplification. The amplifier is realized as a non inverting amplifier. The buffered voltage is applied to an ADC with a resolution of 16 bit and readable by a SPI (serial peripheral interface). Especially the routing of the wires to and from the Hall device

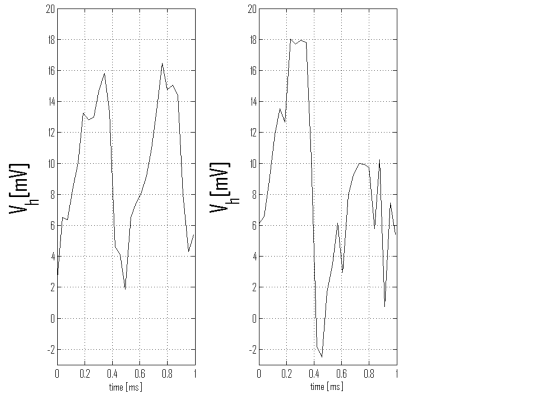


Fig. 5. Experimental result: Demodulated signal without and with DC background signal

is done under the requirements of reduction of EMI aspects. For the sake of completeness the readout electronic should contain an integrator. This may be realized by replacing the second opamp with an offset compensated Miller integrator. In the demonstrator the integration is done in the digital domain like shown in section IV but the advantages related to noise (see section II) will finally suggest the usage of an analog integrator.

## IV. Experimental results

Different measurements are done to verify the ability to suppress the background magnetic flux density. In Fig. 5 a sampled graph of the demodulated Hall voltage is plotted. The modulation frequency is 1kHz. Obviously the second half period is positive, too, like it is derived previously. In the case when no DC-flux density is superposed the detected Hall voltage is about 16mV in the peak. Also an offset is visible of about 2mV. On the right side the influence of a superposed DC signal is measured. The behavior is the same like shown in section II. The DC background flux density causes a drift of about 3.5mV which is added in the first half period and subtracted in the second half period.

In further investigations the measurement are repeated over 20 periods. On the left side these 20 periods are presented. They are measured by a modulation of the active modulation flux density. On the right side this measurement is repeated with a DC background flux density superposition. This superposition is realized by attaching a permanent magnet on the half ferrite core. The DC amplitude is about 3.5mV. The measurements are plotted in fig. 6 in the known form. The results due to the temporal integration are shown in the plots below. Despite the DC amplitude of about 3.5mV the integration result grows similar in each case. After 20 periods the left case results finally at about 5,0V while the result in the second case is about 4,8V. The residual difference of 200mV is caused by statistical effects. If this measurement is repeated frequently a mean value of this difference appears at zero. The deviation is less if more periods are integrated. By this result the

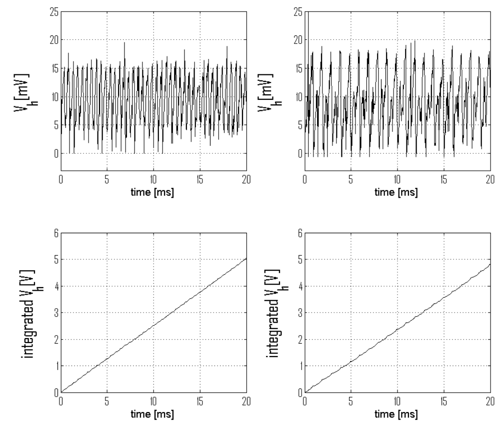


Fig. 6. Experimental result: Hall voltage and integrated signals
left a) Hall voltage
right a) Hall voltage inclusive background signal
left b) integrated Hall voltage
right b) integrated Hall voltage inclusive background signal

suppression effect is validated.

## V. Conclusion and Outlook

A novel and innovative inductive proximity sensor is presented. A principle of effective suppression of background magnetic flux density is theoretical worked out and is described. The suppression effect is validated by measurement results. The smart lock-in receiver is going to be integrated in a standard CMOS process. Due to the availability of small Hall effect devices (e. g. 50$\mu$m x 50$\mu$m) a matrix is going to be developed also. By doing this, research in spatial resolution will be possible.


## VI. Acknowledgment

This work is supported by the chair of Prof. Dr. Ehrhardt. The author wishes also to thank colleagues, especially Klaus Koehler, Dr. Jochen Frey and Tobias Rothermel, of PMDTechnologies GmbH, Siegen and of IMT for their support.


## References


[1] R. Popovic, *Hall Effect Devices*, 2nd ed. IOP Publishing Ltd 2004.

[2] R. Lange, P.Seitz, A.Biber and R. Schwarte, *Time-of-Flight range imaging with a custom sold state imager sensor*, EOS/SPIE International Symposium on Industrial Lasers and Inspection Conference on Laser Metrology and Inspection Munich, Germany, 1999, pp. 180-191, SPIE 3823

[3] Agilent, *Spectrum and Signal Analyzer Measurements and Noise* Application Note 1303,2009

[4] Bowler J. and Johnson M., *Pulsed Eddy-Current Response to a Conducting Half-Space*, IEEE Transaction on Magnetics, Vol. 33, No. 3, May 1997

[5] Banjevic M., Furrer B. and R. S. Popovic, *2D CMOS Integrated Magnetometer Based On The Miniaturized Circular Vertical Hall Device*, Transducer 2009, June 2009

[6] C. C. Enz and G. C. Temes, *Circuit Techniques for Reducing the Effects of Op-Amp Imperfections: Autozeroing, Correlated Double Sampling and Chopper Stabilization*, Proceedings of the IEEE, vol. 84, no. 11, Nov. 1996

[7] Drljaca P. M., Vincent F., Besse P.-A. and R. S. Popovic *Design of planar magnetic concentrators for high sensitivity Hall Devices* Sensors and Actuators A 97-98, 2002